




Cite this: *RSC Adv.*, 2018, 8, 11419

Received 10th January 2018  
 Accepted 7th March 2018

DOI: 10.1039/c8ra00271a

[rsc.li/rsc-advances](http://rsc.li/rsc-advances)

# A novel glutathione-triggered theranostic prodrug for anticancer and imaging in living cells†

Hengrui Zhang and Zhijie Fang \*

A novel theranostic prodrug was designed and synthesized by conjugating a naphthalimide derivative with vitamin D<sub>2</sub> via a disulfide linker. The prodrug featured a highly selective detection process for glutathione (GSH) and showed a red-shifted fluorescence within 30 min. Notably, it also exhibited antitumor activity similar to vitamin D<sub>2</sub> and could be monitored by cellular imaging.

## 1 Introduction

Theranostics is an emerging technology, which is defined as a combination of therapy and diagnostic imaging. Due to its potential to be targeted in a specific manner to the site of disease and reduce or eliminate the possible numerous untoward side effects, theranostics has attracted considerable attention.<sup>1,2</sup> Until now, various imaging techniques have been used for theranostics, such as ultrasound,<sup>3</sup> computed tomography (CT),<sup>4</sup> positron emission tomography (PET)<sup>5</sup> and magnetic resonance imaging (MRI).<sup>6</sup> However, these methods always suffered from some drawbacks, including poor resolution and high costs.<sup>7</sup> In contrast to these conventional methods, naphthalimide-based fluorescence imaging has been developing rapidly due to the advantages of low cost, convenient preparation and high resolution.<sup>8–11</sup>

Biological thiols including glutathione (GSH), cysteine (Cys) and homocysteine (Hcy) always play crucial roles in biological systems.<sup>12–17</sup> An abnormal level of biothiols could be an indicator in many diseases. Given that cancer cells have much higher intracellular glutathione (GSH) concentration than normal cells and tissues, considerable efforts have been devoted to the development of GSH-activatable prodrugs.<sup>18–20</sup> Due to its high sensitivity and rapid response to the disulfide bond, GSH has been broadly utilized as a trigger to cleave the disulfide-containing prodrug and release the active drug. For instance, Zhou *et al.* designed and synthesized a prodrug for cancer treatment by conjugating a naphthalimide derivative and chlorambucil (CLB) via a disulfide linker.<sup>21</sup> Kim *et al.* also conjugated a naphthalimide derivative with camptothecin (CPT) using a disulfide linker, which was highly desirable for *in situ* fluorescence-tracking of cancer chemotherapy.<sup>22</sup>

As an important sterol, vitamin D plays a critical role in calcium homeostasis and bone mineralization and also regulates the proliferation and differentiation of various types of cancer cells.<sup>23–27</sup> However, there has been no report about vitamin D-based theranostic prodrug before. Inspired by this and as continuation of our study, herein, we report a novel theranostic prodrug, which can release vitamin D<sub>2</sub> in the presence of GSH and exhibit distinct fluorescence variation.<sup>28–30</sup>

## 2 Results and discussion

### 2.1 Design and synthesis of prodrug

The theranostic prodrug was designed using three elements. (1) A naphthalimide derivative served as fluorescent reporter, which could be synthesized conveniently from the corresponding 1,8-naphthalic anhydrides by reacting with ethylamine. (2) A disulfide linker that could be cleaved by GSH with high sensitivity and rapid response. (3) An anticancer drug vitamin D<sub>2</sub>, which could be used to regulate gene expression in functions as varied as calcium and phosphate homeostasis, cancer cell growth regulation and differentiation.

Treatment of 4-bromo-1,8-naphthalic anhydride in DMF with sodium azide at room temperature provided the compound 2. It was then reduced with H<sub>2</sub> and 10% Pd/C as catalyst to afford the compound 3. Without any purification, the obtained naphthalic anhydride was condensed with ethylamine to give the key intermediate 4, which was then reacted with triphosgene and 2,2-dithioethanol to afford compound 5. Finally, the desired theranostic prodrug was obtained by reacting compound 5 with vitamin D<sub>2</sub> (Scheme 1). The structure of prodrug was characterized by <sup>1</sup>H NMR, <sup>13</sup>C NMR and HRMS.

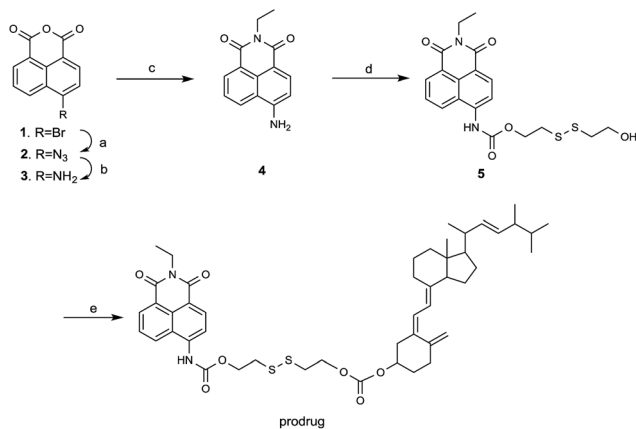
### 2.2 Rapid optical response of the prodrug to GSH

As expected, the prodrug displayed both colorimetric and fluorescence spectral changes upon the addition of GSH. When GSH (200 μM) was added to the PBS/DMSO solution containing

School of Chemical Engineering, Nanjing University of Science & Technology, 200 Xiao Ling Wei, Nanjing 210094, P. R. China. E-mail: zjfang@njust.edu.cn

† Electronic supplementary information (ESI) available: NMR spectra and supplementary data spectra associated with this article can be found. See DOI: 10.1039/c8ra00271a





**Scheme 1** Synthesis of prodrug (a) NaN<sub>3</sub>, DMF, 89.3%; (b) 10% Pd/C, H<sub>2</sub>, DMF, 36 h, 80.1%; (c) ethylamine, ethanol, 4 h, 89.1%; (d) triphosgene, triethylamine, 2-hydroxyethyl disulfide, DCM, 73.2%; (e) triphosgene, triethylamine, vitamin D<sub>2</sub>, 39.1%.

prodrug (10 μM), the absorption peak at 374 nm decreased sharply, and a new band centered at 437 nm could be observed (Fig. 1a). Meanwhile, significant fluorescence turn-on signal changes at 534 nm were observed. Thus, the solution revealed strong yellow fluorescence (Fig. 1b). The fluorescence intensity at 534 nm exhibited a good linear relationship with the GSH concentration and the detection limit was 1.98 μM (Fig. 1c). In addition, the fluorescence intensity of prodrug at 534 nm gradually increased to a plateau within 30 min (Fig. 1d). The time-dependent release efficiency of prodrug in the presence of GSH was displayed in Fig. S1.†

### 2.3 The optical pH range and selectivity of the prodrug for GSH

Similar spectroscopic changes could be observed upon the addition of other free thiols, such as Cys and Hcy. Moreover, the presence of other analytes including amino acids and metal ions induced small or no fluorescence change (Fig. 2a). However, since the concentration of Cys and Hcy was lower than that of GSH in cytoplasm, the possible interference of Cys and Hcy could be neglected. The fluorescence intensity of the prodrug was unaffected over a wide pH range and indicated that the prodrug was quite stable. When GSH (200 μM) was added to the solution, a dramatic fluorescence enhancement could be observed over a pH range of 6–10 (Fig. 2b). These results demonstrated that the prodrug can be applied as a GSH-triggered prodrug in theranostic system with high selectivity over various potential interferons.

### 2.4 Proposed response mechanism of the prodrug for GSH

The proposed mechanism of the prodrug for GSH was displayed by a two-step reaction: cleavage of the disulfide bond and intramolecular cyclization (Scheme 2).<sup>31–33</sup> MS and spectroscopic studies were used to verify the hypothesis. First, the spectra of compound 4 were consistent with that of the prodrug after the treatment with GSH, suggesting that compound 4 was the product (Fig. S2†). Furthermore, ESI-MS titration experiment was carried out to prove the anticipated release of vitamin D<sub>2</sub>. The peaks at *m/z* of 279.07 and 435.35 were observed, which were attributed to [compound 4 + K]<sup>+</sup> and [vitamin D<sub>2</sub> + K]<sup>+</sup> (Fig. S3†). These results were indicative of the cleavage of the

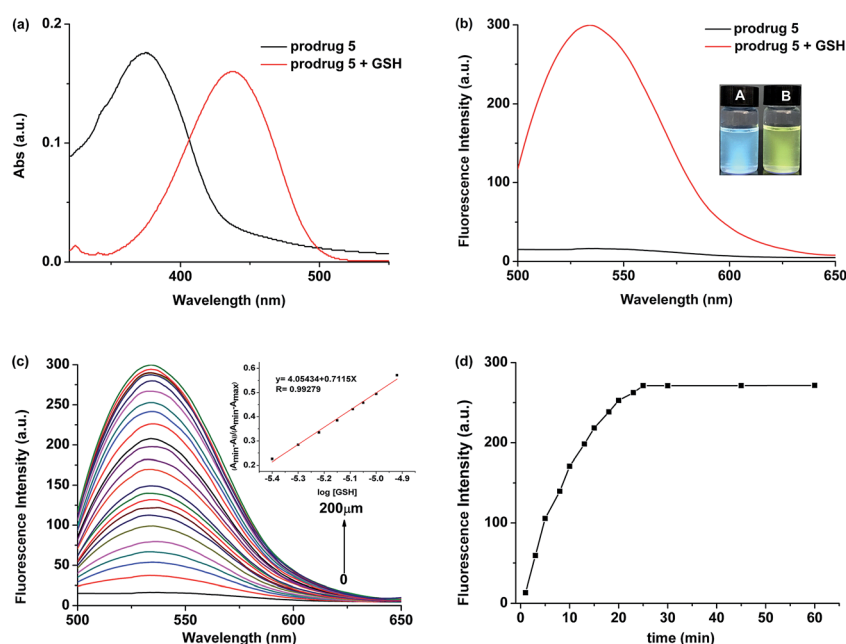


**Fig. 1** (a) UV-Vis spectra changes and (b) fluorescent spectra changes of prodrug (10 μM) before and after incubation with GSH (200 μM) in PBS/DMSO (40 : 60, v/v, pH = 7.4, 10 mM) at 37 °C for 30 min. Fluorescence of prodrug in the absence (A) and in the presence (B) of GSH are inserted. (c) Fluorescence intensity changes of prodrug (10 μM) at 534 nm upon the addition of different concentrations of GSH in PBS. Inset: the linear relationship between fluorescent intensity and GSH concentration (d) time dependence of fluorescence intensity of prodrug in the presence of GSH.



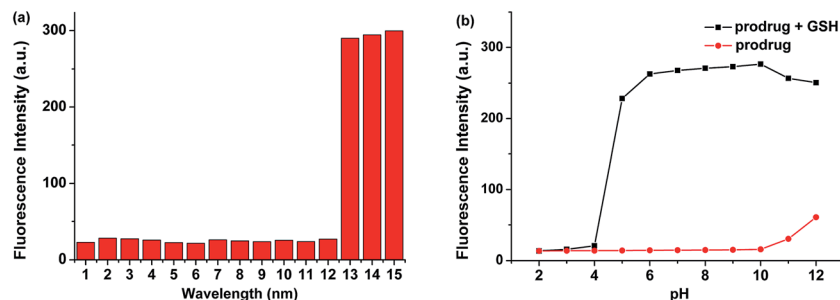
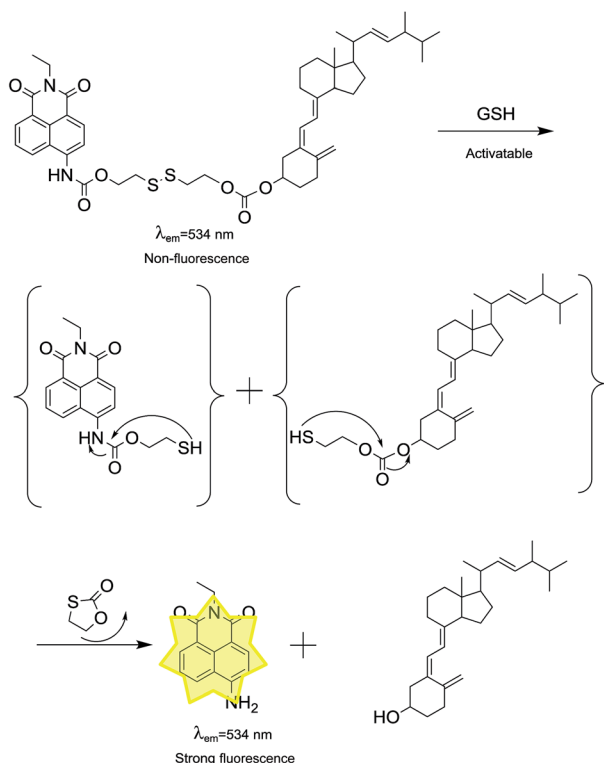


Fig. 2 (a) Fluorescent spectra responses of prodrug for various analytes (1–14 represent: (1)  $\text{Al}^{3+}$ , (2)  $\text{Cu}^{2+}$ , (3)  $\text{NO}_3^-$ , (4)  $\text{SO}_4^{2-}$ , (5) Leu, (6) Tyr, (7) Arg, (8) Glu, (9) Lys, (10) Thr, (11) Ser, (12) Hcy, (13) Cys, (14) GSH). (b) The pH effect of the fluorescence intensity of prodrug in the absence and in the presence of GSH. Each spectrum was collected after 30 min of mixing each analyte with prodrug in PBS/DMSO (40 : 60, v/v, pH = 7.4, 10 mM) at 37 °C.



Scheme 2 Proposed response mechanism of the prodrug for GSH.

disulfide group and the production of fluorophore and vitamin  $\text{D}_2$  in the sensing reaction.

### 2.5 Antitumor activity evaluation and live cell imaging

The prodrug displayed good biocompatibility to HEK 293T cells (Fig. S4†). Inspired by above results, we further investigated the practicability of the prodrug in biological systems by carrying out antitumor activity and bioimaging experiments. To determine the antitumor activity, vitamin  $\text{D}_2$ , compound 5 and prodrug were first incubated with HeLa cells and then evaluated by using typical MTT assays. Prodrug and vitamin  $\text{D}_2$  showed similar antitumor activity against HeLa cell lines, while compound 5 showed low activity for living cells (Fig. 3). Then,

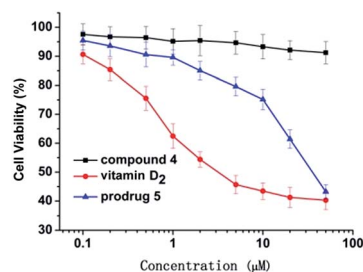


Fig. 3 Antitumor activity of compound 5, vitamin  $\text{D}_2$  and prodrug on HeLa cancer cells.

the cellular uptake and intracellular localization of prodrug were investigated using a fluorescence microscope. When HeLa cells were incubated with the prodrug for 30 min, weak fluorescence from prodrug was observed, indicating that the prodrug was sufficiently activated by the high concentration of GSH in cancer cells. To demonstrate the role of the GSH presented in disulfide cleavage, additional 1.0 mM prodrug was added to HeLa cells and an enhanced fluorescence was observed (Fig. 4). These results were fully consistent with the design expectations

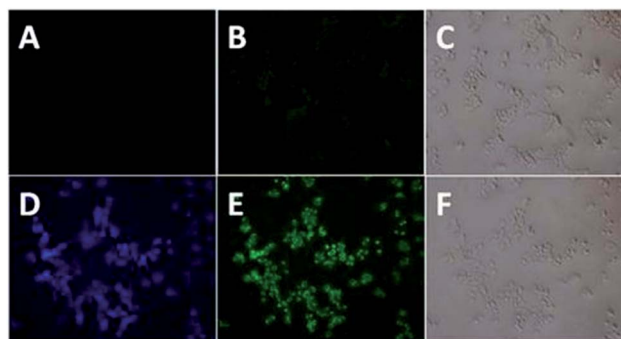


Fig. 4 The upside: images of HeLa cells incubated only with the prodrug (10  $\mu\text{M}$ ) for 30 min; (A) fluorescence image at the blue channel, (B) fluorescence image at the green channel, (C) bright-field image. The downside: images of HeLa cells incubated with GSH (1.0 mM) for 30 min, then treated with the prodrug (10  $\mu\text{M}$ ) for 30 min. (D) Fluorescence image at the blue channel, (E) fluorescence image at the green channel, (F) bright-field image.



and suggested that the prodrug can be used to monitor the drug release process in cancer cells.

### 3 Conclusion

In summary, we developed a novel theranostic prodrug by conjugating the naphthalimide chromophore and vitamin D<sub>2</sub> via a disulfide bond. This prodrug can discriminate GSH from a wide array of amino acids and ions. It also can be used to quantify GSH with a detection limit as low as 1.98 μM and rapid detection process for GSH within 30 min. In addition, this prodrug displayed similar antitumor activity with vitamin D<sub>2</sub> and can be used for intracellular fluorescence imaging. Overall, this prodrug can be used as a valuable research tool for GSH-activatable drug delivery system and can be easily monitored by cellular imaging.

### 4 Experimental procedures

#### 4.1 Materials and apparatus

All chemical reagents and solvents were purchased from commercial suppliers and used without further purification. <sup>1</sup>H and <sup>13</sup>C NMR spectra were obtained on Bruker Avance III 500 MHz spectrometer. HRMS spectra were obtained on a Bruker ApexII by means of the ESI technique. Absorption and fluorescence spectra were obtained on Lambda 35 UV-Vis spectrophotometer and a Shimadzu RF-5301PC Fluorescence Spectrometer, respectively. All titrations were carried out in PBS/DMSO solution (40 : 60, v/v, pH = 7.4).

#### 4.2 Synthesis of compound 4

Initially, 4-bromo-1,8-naphthalic anhydride (10 g, 36.1 mmol) was dissolved in DMF (50 mL) and then, NaN<sub>3</sub> (3.5 g, 53.8 mmol) was added into the solution. The mixture was stirred overnight and added to water to obtain yellow precipitate. The precipitate was filtered and dried to obtain compound 2 (7.6 g, 89.3%).

Compound 2 (5 g, 20.8 mmol) was dissolved in DMF (50 mL), followed by the addition of 10% Pd/C (400 mg). Then, the mixture was stirred under H<sub>2</sub> atmosphere at room temperature for 36 h. After filtration, water was added into the solution to obtain yellow precipitate. The precipitate was filtered and dried to give compound 3 (3.5 g, 80.1%).

Compound 3 (3 g, 14.1 mmol) was dissolved in ethanol (160 mL), following which ethylamine (4 mL) was added dropwise. The mixture was refluxed for 4 h and then added to water to obtain precipitate. The precipitate was filtered and dried to yield compound 4 (3.7 g, 89.1%). <sup>1</sup>H NMR (500 MHz, DMSO): δ 8.51 (1H, d, *J* = 8.1 Hz), 8.30 (1H, d, *J* = 7.2 Hz), 8.10 (1H, d, *J* = 8.4 Hz), 7.65 (1H, m), 7.33 (2H, s), 6.76 (1H, d, *J* = 8.4 Hz), 3.97 (2H, d, *J* = 7.1 Hz), 1.11 (3H, t, *J* = 7.0 Hz) ppm; <sup>13</sup>C NMR (126 MHz, DMSO): δ 162.58, 152.11, 133.30, 130.34, 128.89, 123.37, 121.27, 118.82, 107.36, 33.68, 12.78 ppm.

#### 4.3 Synthesis of compound 5

Compound 4 (0.5 g, 1.1 mmol) and triphosgene (1.2 g, 4.0 mmol) were dissolved in dichloromethane (30 mL) and

stirred for 0.5 h at 0 °C, following which triethylamine (1.7 mL) was added and stirred for another 60 min. Then, 2-hydroxyethyl disulfide (2.8 mL) was added and stirred at room temperature to obtain yellow precipitate. The precipitate was filtered and dried to give compound 5 (1.3 g, 73.2%). <sup>1</sup>H NMR (500 MHz, DMSO): δ 10.29 (1H, s), 8.64 (1H, d, *J* = 8.5 Hz), 8.40 (2H, m, *J* = 7.7 Hz), 8.13 (1H, d, *J* = 8.2 Hz), 7.76 (1H, s), 4.49 (2H, t, *J* = 6.4 Hz), 4.05 (2H, d, *J* = 7.1 Hz), 3.69 (2H, d, *J* = 6.4 Hz), 3.14 (2H, t, *J* = 6.4 Hz), 2.90 (2H, t, *J* = 6.4 Hz), 1.22 (3H, t, *J* = 7.0 Hz) ppm; <sup>13</sup>C NMR (126 MHz, DMSO): δ 162.58, 162.02, 153.25, 139.97, 130.89, 130.14, 128.60, 127.58, 125.62, 123.15, 121.53, 117.52, 116.44, 62.48, 58.92, 40.62, 36.22, 34.08, 12.58 ppm.

#### 4.4 Synthesis of prodrug

Compound 5 (0.2 g, 0.5 mmol) and triphosgene (0.62 g, 2.01 mmol) were dissolved in dichloromethane (30 mL) and stirred for 0.5 h at 0 °C, following which triethylamine (1.69 mL) was added and stirred for another 60 min. Then, vitamin D<sub>2</sub> (0.2 g, 0.05 mmol) was added and stirred at room temperature until the reaction was complete. Finally, the mixture was concentrated under reduced pressure and purified by column chromatography on silica gel to obtain the prodrug (0.15 g, 39.1%). <sup>1</sup>H NMR (500 MHz, CDCl<sub>3</sub>): δ 8.62 (1H, m, *J* = 13.2 Hz), 8.33 (1H, m, *J* = 8.4 Hz), 7.84 (1H, s), 7.80 (1H, m), 6.19 (1H, d, *J* = 11.2 Hz), 5.98 (1H, d, *J* = 11.2 Hz), 5.17 (1H, m, *J* = 7.4 Hz), 5.04 (1H, s), 4.89 (1H, m), 4.55 (1H, t, *J* = 6.1 Hz), 4.51 (1H, m), 4.24 (1H, q, *J* = 7.1 Hz), 3.15 (2H, m), 2.81 (1H, m), 2.60 (1H, m, *J* = 13.4 Hz), 2.40 (1H, m, *J* = 6.2 Hz), 2.21 (1H, m), 2.08 (2H, m), 1.89 (1H, m), 1.75 (3H, m), 1.52 (3H, m), 1.37 (5H, m), 1.05 (2H, m), 0.96 (6H, m), 0.52 (2H, s) ppm; <sup>13</sup>C NMR (126 MHz, CDCl<sub>3</sub>): δ 162.96, 162.46, 153.53, 152.12, 143.01, 141.77, 138.09, 134.59, 132.49, 131.17, 130.22, 127.87, 125.54, 122.12, 116.54, 112.20, 75.17, 64.62, 62.28, 55.43, 44.81, 41.82, 40.99, 39.39, 36.55, 35.73, 34.51, 32.12, 30.83, 28.06, 26.80, 22.58, 21.22, 20.13, 18.84, 16.62, 12.39, 11.26 ppm. HRMS [M + H]<sup>+</sup>: calcd for C<sub>48</sub>H<sub>62</sub>N<sub>2</sub>O<sub>7</sub>S<sub>2</sub> 842.3998, found 843.4071.

#### 4.5 Absorption and fluorescence spectroscopy

Stock solution of prodrug, vitamin D<sub>2</sub> and compound 4 (2.0 × 10<sup>-3</sup> M) was prepared in DMSO. Individually, stock solutions (1 mM) of the analytes Cys, Hcy, GSH, leucine (Leu), tyrosine (Tyr), arginine (Arg), glutamic acid (Glu), lysine (Lys), threonine (Thr), and serine (Ser) were prepared in ultrapure water. For a typical optical study, the prodrug (10 μM) solution in PBS/DMSO (40 : 60, v/v, pH = 7.4, 10 mM) was prepared. Then, 3.0 mL of the solution was placed in a quartz cuvette at room temperature. For fluorescent measurements, slit width was set at *d*<sub>ex</sub> = 3 nm, *d*<sub>em</sub> = 3 nm.

#### 4.6 Cell incubation and imaging

HeLa cells used in this study were purchased from Cbioer Biosciences Co., Ltd. (Nanjing, China). HEK 293T cells used in this study were purchased from Chinese Academy of Sciences (Shanghai, China). HeLa cells were cultured in Dulbecco's modified Eagle's medium (DMEM) supplemented with 10% fetal bovine serum (FBS) at 37 °C in an atmosphere of 5% CO<sub>2</sub>.





The images of cells were visualized and photographed by a fluorescence microscope (Nikon, Japan). In the experiment of cell imaging, cells were incubated with 10  $\mu\text{M}$  of prodrug (with 0.2% DMSO, v/v) for 30 min at 37  $^{\circ}\text{C}$ , washed with pre-warmed PBS thrice and then imaged. For GSH treated experiments, the HeLa cells were pretreated with 1.0 mM GSH at 37  $^{\circ}\text{C}$  for 30 min, washed with PBS three times, and then incubated with 10  $\mu\text{M}$  prodrug at 37  $^{\circ}\text{C}$  for 30 min. Cell imaging was then carried out after washing cells with prewarmed PBS.

## Conflicts of interest

There are no conflicts to declare.

## Notes and references

- 1 A. Gharatape and R. Salehi, *Eur. J. Med. Chem.*, 2017, **138**, 221–233.
- 2 S. S. Kelkar and T. M. Reineke, *Bioconjugate Chem.*, 2011, **22**, 1879–1903.
- 3 J. Chen, S. Ratnayaka, A. Alford, V. Kozlovskaya, F. Liu, B. Xue, K. Hoyt and E. Kharlampieva, *ACS Nano*, 2017, **11**, 3135–3146.
- 4 S. Moendarbari, R. Tekade, A. Mulgaonkar, P. Christensen, S. Ramezani, G. Hassan, R. Jiang, O. K. Öz, Y. Hao and X. Sun, *Sci. Rep.*, 2016, **6**, 20614–20622.
- 5 J. Guo, H. Hong, G. Chen, S. Shi, T. R. Nayak, C. P. Theuer, T. E. Barnhart, W. Cai and S. Gong, *ACS Appl. Mater. Interfaces*, 2014, **6**, 21769–21779.
- 6 J. Kaur, Y. Tsvetkova, K. Arroub, S. Sahnoun, F. Kiessling and S. Mathur, *Chem. Biol. Drug Des.*, 2017, **89**, 269–276.
- 7 M. G. Sikkandhar, A. M. Nedumaran, R. Ravichandar, S. Singh, I. Santhakumar, Z. C. Goh, S. Mishra, G. Archunan, B. Gulyás and P. Padmanabhan, *Int. J. Mol. Sci.*, 2017, **18**, 1036–1063.
- 8 K. H. Hong, D. I. Kim, H. Kwon and H. J. Kim, *RSC Adv.*, 2013, **4**, 978–982.
- 9 S. Banerjee, E. B. Veale, C. M. Phelan, S. A. Murphy, G. M. Tocci, L. J. Gillespie, D. O. Frimannsson, J. M. Kelly and T. Gunnlaugsson, *Chem. Soc. Rev.*, 2013, **42**, 1601–1618.
- 10 L. Rong, C. Zhang, Q. Lei, H. L. Sun, S. Y. Qin, J. Feng and X. Z. Zhang, *Chem. Commun.*, 2015, **51**, 388–390.
- 11 H. S. Kim, W. Y. Song and H. J. Kim, *Org. Biomol. Chem.*, 2015, **13**, 73–76.
- 12 S. Zhang, C. N. Ong and H. M. Shen, *Cancer Lett.*, 2004, **208**, 143–153.
- 13 X. Chen, Y. Zhou, X. Peng and J. Yoon, *Chem. Soc. Rev.*, 2010, **39**, 2120–2135.
- 14 J. Lačná, F. Foret and P. Kubáň, *Electrophoresis*, 2016, **38**, 203–222.
- 15 Q. Sun, D. Sun, L. Song, Z. Chen, Z. Chen, W. Zhang and J. Qian, *Anal. Chem.*, 2016, **28**, 177–221.
- 16 L. Song, H. Tian, X. Pei, Z. Zhang, W. Zhang and J. Qian, *RSC Adv.*, 2015, **5**, 59056–59061.
- 17 J. Qian, L. Song, Q. Sun, N. Wang, Z. Chen and W. Zhang, *Anal. Methods*, 2015, **7**, 10371–10375.
- 18 M. H. Lee, J. H. Han, P. S. Kwon, S. Bhuniya, J. Y. Kim, J. L. Sessler, C. Kang and J. S. Kim, *J. Am. Chem. Soc.*, 2012, **134**, 1316–1322.
- 19 F. Kong, Z. Liang, D. Luan, X. Liu, K. Xu and B. Tang, *Anal. Chem.*, 2016, **88**, 6450–6456.
- 20 X. Wu, X. Sun, Z. Guo, J. Tang, Y. Shen, T. D. James, T. He and W. Zhu, *J. Am. Chem. Soc.*, 2014, **136**, 3579–3588.
- 21 J. Wu, R. Huang, C. Wang, W. Liu, J. Wang, X. Weng, T. Tian and X. Zhou, *Org. Biomol. Chem.*, 2013, **11**, 580–585.
- 22 M. H. Lee, Z. Yang, C. W. Lim, Y. H. Lee, S. Dongbang, C. Kang and J. S. Kim, *Chem. Rev.*, 2013, **113**, 5071–5109.
- 23 K. K. Deeb, D. L. Trump and C. S. Johnson, *Nat. Rev. Cancer*, 2007, **7**, 684–700.
- 24 J. L. Costa, P. P. Eijk, M. A. van de Wiel, D. ten Berge, F. Schmitt, C. J. Narvaez, J. Welsh and B. Ylstra, *BMC Genomics*, 2009, **10**, 499–504.
- 25 G. Jones, *Endocrinol. Metab. Clin. North Am.*, 2010, **39**, 447–472.
- 26 X. Gu, Q. Chen and Z. Fang, *Dyes Pigm.*, 2017, **139**, 334–343.
- 27 T. Zhang, T. Wang and Z. Fang, *RSC Adv.*, 2016, **6**, 18357–18363.
- 28 L. Li and Z. Fang, *Spectrosc. Lett.*, 2015, **48**, 578–585.
- 29 W. Guo, Z. Fang, H. Li and Y. Liu, *J. Chem. Res.*, 2014, **38**, 231–235.
- 30 H. Li, Z. Fang, H. Dai, H. Zhang and Y. Liu, *J. Chem. Res.*, 2015, **39**, 368–372.
- 31 Y. Zhang, Q. Yin, J. Yen, J. Li, H. Ying, H. Wang, Y. Hua, E. J. Chaney, S. A. Boppart and J. Cheng, *Chem. Commun.*, 2015, **51**, 6948–6951.
- 32 M. Ye, X. Wang, J. Tang, Z. Guo, Y. Shen, H. Tian and W. H. Zhu, *Chem. Sci.*, 2016, **7**, 4958–4965.
- 33 Z. Yang, J. H. Lee, H. M. Jeon, J. H. Han, N. Park, Y. He, H. Lee, K. S. Hong, C. Kang and J. S. Kim, *J. Am. Chem. Soc.*, 2013, **135**, 11657–11662.

